Available online at www.sciencedirect.com
SCIENCE DIRECT®
C. R. Chimie 8 (2005) 1392–1399
COMPTES RENDUS CHIMIE
http://france.elsevier.com/direct/CRAS2C/

Account / Revue

The experimental charge density in transition metal compounds

Riccardo Bianchi [a], Giuliana Gervasio [b,*], Domenica Marabello [b]

[a] *CNR-Istituto di Scienze e Tecnologie Molecolari, via Golgi 19, 20133 Milan, Italy*
[b] *Dipartimento di Chimica I.F.M., Via P. Giuria 7, 10125 Turin, Italy*

Received 31 March 2004; accepted 16 December 2004

Available online 25 May 2005

Abstract

Today, the experimental charge density of transition metal compounds can be determined with a good degree of reliability and analyzed with the quantum theory of atoms in molecules in order to better characterize the atomic interaction. Here, we present a short summary of the main topological results obtained with this technique on $Mn_2(CO)_{10}$, $Co_2(CO)_6(\mu\text{-}CO)(\mu\text{-}C_4O_2H_2)$, $KMnO_4$ and $KClO_4$ compounds. ***To cite this article: R. Bianchi et al., C. R. Chimie 8 (2005)***.

Résumé

De nos jours, la densité de charge des composés de métaux de transition peut être déterminée expérimentalement, avec un bon degré de fiabilité, et analysée à l'aide de la théorie quantique des atomes dans la molécule, afin de mieux caractériser l'interaction atomique. Nous présentons ici un court résumé des principaux résultats topologiques obtenus avec cette technique sur les composés $Mn_2(CO)_{10}$, $Co_2(CO)_6(\mu\text{-}CO)(\mu\text{-}C_4O_2H_2)$, $KMnO_4$ et $KClO_4$. ***Pour citer cet article : R. Bianchi et al., C. R. Chimie 8 (2005)***.

Keywords: Charge density; Transition metal; Multipole analysis; Topology; QTAIM

Mots clés : Densité de charge ; Métaux de transition ; Analyse multipole ; Topologie ; QTAIM

1. Introduction

The charge density in transition metal compounds is of great interest owing to the importance of these systems in catalysis, in solid-state chemistry, and in a large number of key biological processes. Today, the charge density of such compounds can be determined with a good degree of accuracy both theoretically and experimentally from single crystal X-ray diffraction. Recently [1], an exhaustive review has been published on charge density analysis.

However, the calculation of theoretical charge densities on systems with a large number of electrons shows

* Corresponding author.
E-mail addresses: riccardo.bianchi@istm.cnr.it (R. Bianchi), giuliana.gervasio@unito.it (G. Gervasio), domenica.marabello@unito.it (D. Marabello).

1631-0748/$ - see front matter © 2005 Académie des sciences. Published by Elsevier SAS. All rights reserved.
doi:10.1016/j.crci.2004.12.015

often problems that are mainly connected to the large number of two-electron integrals and relativistic effects.

On the experimental side, the technical improvement of diffractometers and of new devices for data collection at low temperature, and the development of powerful programs based on the use of the aspherical atoms formalism, allow to obtain experimental charge densities with a good degree of reliability. Furthermore, the quantum theory of atoms in molecules (QTAIM) [2] applied to experimental and theoretical charge densities permits a quantitative characterization of the chemical bond for many transition metal compounds appeared in the literature.

2. Determination and topological analysis of the experimental charge density

In the X-ray analysis of crystal structure, the independent atom model (IAM), where the atom is considered isolated with spherical symmetry, is a rule used. The superposition of spherical free-atom densities, each centered at atomic positions, is called the pro-density. The pro-density describes the major part of the charge density of a molecule (or crystal) and only a relatively small part of the electron density of an atom, located in the valence shell, is involved in chemical interactions. When atoms form chemical bonds, the valence shell expands or contracts with variation of atomic charge and valence density is aspherically deformed. In this case, the spherical core and the valence deformation density of each pseudo (or aspherical) atom p is expressed by a sum of terms defined by $C_{\mathrm{plm}}\, R_{\mathrm{p}}(r)\, Y_{\mathrm{lm}}(\theta, \phi)$ (multipole expansion), where C_{nlm} is a population parameter, $R_{\mathrm{p}}(r)$ is a radial function of Slater type or a fixed linear combination of exponentials and $Y_{\mathrm{lm}}(\theta, \phi)$ is a surface spherical harmonic [3,4].

The VALRAY [5] and XD [6] are two programs that apply flexible, nucleus centered, pseudo-atom multipole expansions of charge densities in crystals, as described above. The C_{nlm} population parameters are adjustable parameters that can be refined by the least-squares method on the basis of observed structure amplitudes. Thus at the end of refinement, the multipole charge density can be analyzed using topological methods. The last versions of the VALRAY and XD program packages include also the calculation of an extensive set of electrostatic properties from X-ray data: electrostatic potentials, electric fields, charge densities and electric field gradients etc. Moreover, they include a procedure for a complete topological analysis of the experimental charge density [7]. In this work all the multipole refinements on F^2 were performed using the atom-centered multipole model by Stewart [3].

The topology of the charge density, $\rho(\mathbf{r})$, and its Laplacian, $\nabla^2\rho(\mathbf{r})$, is related to chemical concepts by the QTAIM. [2] The definition of the chemical bond is based on the existence of a bond critical point (BCP) along a line of maximum density (bond path), linking the nuclei of neighboring atoms. At the BCP, the gradient of density vanishes and the sign of the Laplacian is determined by the relationship, $\nabla^2\rho_{\mathrm{BCP}} = \lambda_1 + \lambda_2 + \lambda_3$ ($\lambda_1 < 0$, $\lambda_2 < 0$ and $\lambda_3 > 0$ are the three non-zero eigenvalues of the Hessian matrix). The values of λ_1 and λ_2 measure the degree of the $\rho(\mathbf{r})$ contraction towards the BCP, while λ_3 gives the $\rho(\mathbf{r})$ contraction towards each of the bonded nuclei. Extremes in $\rho(\mathbf{r})$ and in $\nabla^2\rho(\mathbf{r})$ are labeled by giving the pair of values (ω, σ): ω denotes the rank that is equal to the number of non-zero eigenvalues and σ denotes the number of positive eigenvalues minus the number of the negative ones. On the basis of the Laplacian sign, the bonding interactions have been divided into two great categories [2]: when $\nabla^2\rho_{\mathrm{BCP}} < 0$ the interaction is denoted as 'shared' while when $\nabla^2\rho_{\mathrm{BCP}} > 0$ the interactions are 'closed shell'[1]. In the first category fall the typical covalent and polar-covalent bonds, in the second the ionic and the van der Waals bonds.

An additional straightforward criterion for the characterization of chemical bond is provided by the local charge energy density, $H_{\mathrm{BCP}} = G_{\mathrm{BCP}} + V_{\mathrm{BCP}}$, where G_{BCP} and V_{BCP} indicate, respectively, the values of the kinetic and potential energy density at the BCP, and they can be estimated from the experimental $\rho(\mathbf{r})$ using the approximate functionals proposed by Kirzhnits [8], Abramov [9] and Espinosa et al. [10]. A negative H_{BCP} value is indicative of a prevalent potential energy density on kinetic energy density and thus of a covalent character of the interaction. On the contrary, a positive H_{BCP} value reveals a prevalence of the kinetic energy density, typical behavior of the ionic and van der Waals interactions [11,12].

[1] The 'shared' and 'closed-shell' terminology are referred exclusively to the shared or not-shared valence shells of the two interacting atoms.

Recently, Espinosa et al. [13] proposed a classification of the atomic interactions dividing them into three characteristic regions: *pure* closed shell (region I, $\nabla^2\rho_{BCP} > 0$, $H_{BCP} > 0$), *transit* closed shell (region II, $\nabla^2\rho_{BCP} > 0$, $H_{BCP} < 0$) and *pure* shared shell (region III, $\nabla^2\rho_{BCP} < 0$, $H_{BCP} < 0$). The boundaries among regions I, II, and III are defined by $H_{BCP} = 0$ (i.e. $|V_{BCP}|/G_{BCP} = 1$) and by $\nabla^2\rho_{BCP} = 0$ (i.e. $|V_{BCP}|/G_{BCP} = 2$). Inside the region I the bond degree parameter (BD = H_{BCP}/ρ_{BCP}) is an index of non-covalent interaction and it is indicated as softening degree (SD) *per* charge density unit at BCP; the weaker the interaction, the greater the SD magnitude. In the regions II and III the BD parameter measures the covalence degree (CD) of any pair-wise interaction; the stronger the interaction, the greater the CD magnitude. For example, a typical covalent bond lies inside the region III (*pure* shared shell), while an ionic bond in the region I (*pure* closed shell).

Further information on the bond properties can be obtained from the number and properties of the local $\nabla^2\rho(\mathbf{r})$ maxima and minima in the valence shell charge concentration (VSCC) of the bonded atoms: these features depend on the chemical environment of each atom.

3. Charge-density studies of transition-metal compounds

The work of our group in this field began in the late 1990s with a paper on the experimental charge density of an organic mesoionic compound (4-cyano-imidazolium-5-olate) [14], joining different experiences in the crystallographic field [15–22]. For the 4-cyanoimidazolium-5-olate a comparison was made of the electrostatic potential between experiment and theory for the isolated molecule. A good agreement between experiment and theory was obtained for the atomic charges and molecular dipole moment (μ_{exp} = 2.3(3) e Å, $\mu_{HF/6-31G^{**}}$ = 2.40 e Å). Fig. 1a, b show the Laplacian and the electrostatic potential maps, respectively, in the molecular plane.

The results obtained for the mesoionic compound stimulated us to direct our research towards the study of the charge density in organometallic compounds. The complex $Mn_2(CO)_{10}$ was the first system studied

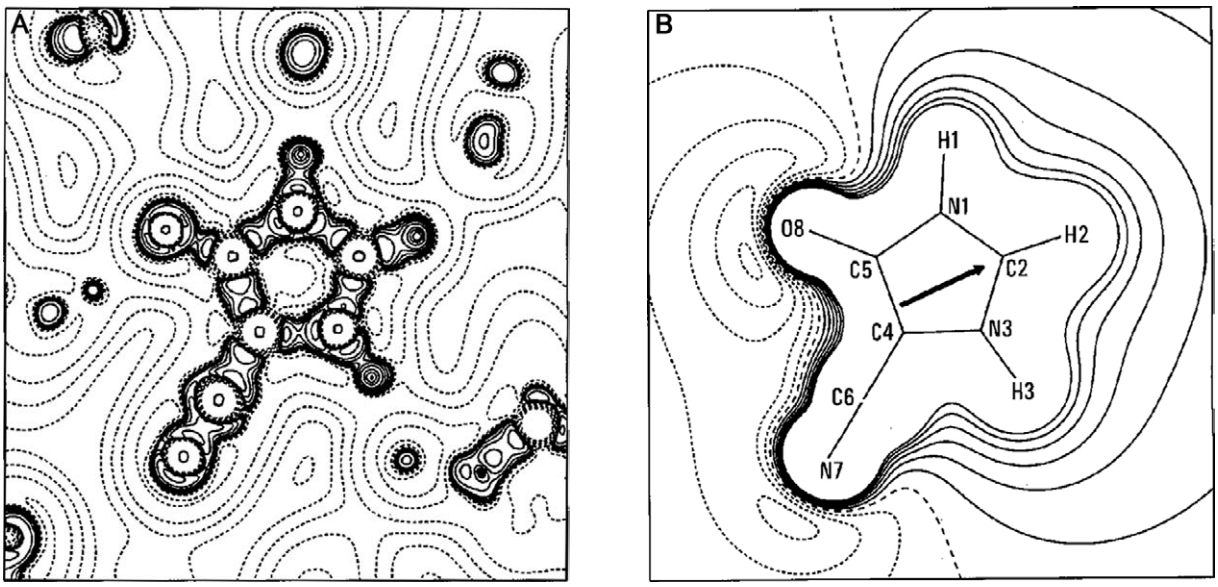

Fig. 1. (**A**) Laplacian of the charge density in the plane of 4-cyanoimidazolium-5-olate molecule. The absolute values of contours (in a. u.) increase from the outermost one inwards in steps of 2×10^n, 4×10^n and 8×10^n, with n beginning at –3 and in steps of 1. Positive values of $\nabla^2\rho$ are denoted by dashed lines, negative values by solid lines. (**B**) Multipole electrostatic potential map for molecule. The contours are at intervals of 0.05 e Å^{-1}; solid lines positive, short dashed lines negative, large dashed line zero contour. The arrow originates at the molecular center of mass and indicates the direction of the molecular dipole moment.

[23,24]. The three bonding structures, proposed at that time, are shown in Scheme 1.

Other researchers analyzed the charge density and chemical bonding of this compound from the theoretical and experimental point of view [25]. No clear probe, however, of the existence of a direct Mn–Mn bond was achieved and also *crossed* bonds between Mn and the CO molecules linked to the other manganese atom have not been excluded (Scheme 1b, c). We collected accurate X-ray data at low temperature (120 K) from a single $Mn_2(CO)_{10}$ crystal, carried out the multipole refinement with VALRAY program and interpreted the experimental $\rho(\mathbf{r})$ with the QTAIM. The topological analysis showed the presence of a bond between the two manganese atoms and none of the hypothesized *crossed* bonds were found, confirming the bonding Scheme 1a.

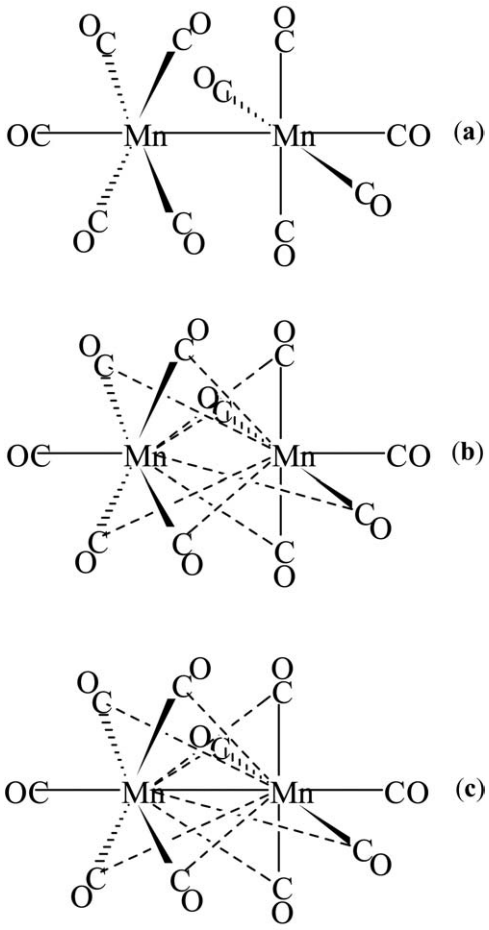

Scheme 1. Bonding structures proposed for $Mn_2(CO)_{10}$.

The charge density (with bond paths and BCP superimposed) and Laplacian maps, nearly in the plane containing the two Mn atoms, one axial and two equatorial COs, are shown in Fig. 2.

As it is shown in Fig. 2b, the C–O bonds have large negative $\nabla^2\rho_{BCP}$ (–40 e Å^{-5} av.), while the Mn–Mn and Mn–C bonds have positive $\nabla^2\rho_{BCP}$ (0.815 and 14.0 e Å^{-5} av., respectively). Therefore, the C–O bonds are classified as 'shared' interactions, while the metal–metal and metal–ligand bonds belong to the 'closed-shell' type and exhibit different topological features with respect to the typical covalent bonds. The low negative H_{BCP} values of Mn–Mn (–0.031 hartree Å^{-3}) and Mn–C (–0.28 hartree Å^{-3} av.) bonds is also indicative of their little covalent character. A preliminary scheme was proposed for classification of the bonds present in organometallic complexes, utilizing the few data at disposal at that time [26–28] (see Fig. 3).

On the basis of the topological and energetic parameters, this scheme places the metal–metal bonds between ionic and covalent bonds, attributing to them a peculiar 'metallic' feature. The Mn–C bonds can be better described analyzing the Laplacian maxima and minima of the Mn and C atoms: a $\nabla^2\rho_{BCP}$ maximum was found on each C-atom pointing toward an hole in the Mn atom, showing the 'dative' nature of this bond type [24,29].

The existence of the metal–metal bond in complexes with bridging ligands is another debated problem. For example, three bonding schemes have been proposed for $Co_2(CO)_8$ with a straight or curved Co–Co bond or with the lacking of a direct Co–Co bond [30]. For this reason we have taken into account a similar dicobalt carbonyl complex containing one bridging CO and one bridging γ-lactonic ring, of formula $Co_2(CO)_6(\mu\text{-}CO)(\mu\text{-}C_4O_2H_2)$ [28,31–33] (see Fig. 4a).

Two polymorphs, one orthorhombic and the other triclinic, of this compound have been topologically analyzed, starting from the multipole-refined charge density. In both cases a direct Co–Co bond path have been found. On the contrary, other authors [34,35] have not found a direct metal–metal bond in their charge density studies of transition metal clusters with supported metal–metal interactions. Furthermore, theoretical calculations on $Co_2(CO)_8$ and $Co_4(CO)_{12}$ [36] agree with our experimental results.

For the two crystal phases of the $Co_2(CO)_6(\mu\text{-}CO)(\mu\text{-}C_4O_2H_2)$ complex, the topological properties of metal–

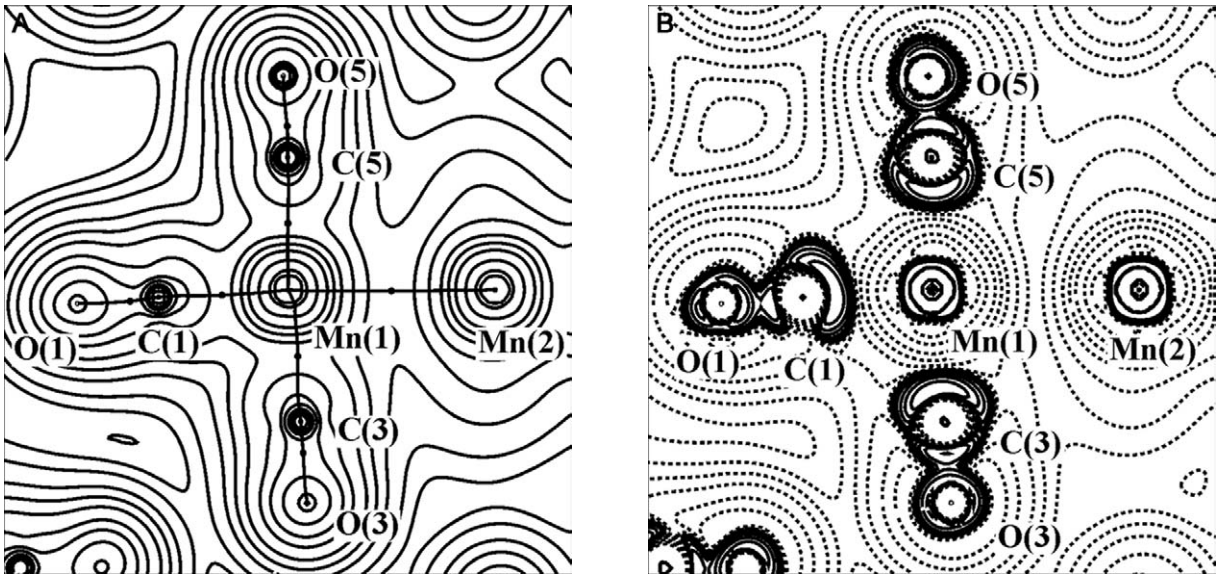

Fig. 2. Experimental charge density (**A**) and its Laplacian (**B**) of $Mn_2(CO)_{10}$ molecule, in the plane defined by Mn(1), Mn(1A) and C(3) atoms. The contours are as in Fig. 1a.

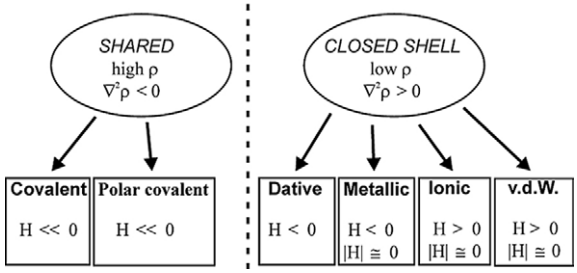

Fig. 3. Classification of bonds on the basis of topological parameters ρ_{BCP}, $\nabla^2\rho_{BCP}$ and H_{BCP}.

metal, metal–ligand and C–O bonds have been found similar to those obtained in previous studies, thus supporting the bond classification of organometallic compounds above illustrated. The topological data derived for the Co–Co bond are collected in Table 1; it shows that ρ_{BCP} is inversely proportional to the Co–Co bond distance. Furthermore, it was evidenced a flat charge density distribution around the BCP of the metal–metal bond (see Figs. 2b and 4b) and a small prevalence of potential energy density (V_{BCP}) over the kinetic energy density (G_{BCP}) ($H_{BCP} < 0$, but near to 0).

The study of the two polymorphs of $Co_2(CO)_6(\mu\text{-}CO)(\mu\text{-}C_4O_2H_2)$ has allowed to detect, even in presence of heavy atoms, the weak intermolecular interactions (O···O, H···O) responsible for the two crystal packings (see for example Fig. 4c); in the orthorhombic form, the hydrogen bonds involving the *lactone* ligand are the driving forces for the crystal packing, while in the triclinic form the O···O van der Waals interactions are predominant.

The compounds so far examined have the metal atoms in a formal zero oxidation state. It is known that the behavior of transition metals in a high oxidation state differs from that at zero oxidation state. For this reason the charge density study of $KMnO_4$ has been undertaken and compared with that of the isomorphous $KClO_4$ [37], containing the non-metal Cl atom in the same chemical environment of the Mn atom. The topological results were also rationalized using the classification recently proposed by Espinosa et al. [13]. According to this classification the K–O and Cl–O bonds have a pure ionic and covalent character, respectively. The Mn–O bonds show an intermediate behavior and fall in the *transit* CS region (Fig. 5). These results are also in good agreement (even on a quantitative level) with those obtained from fully periodic Hartree–Fock and density functional calculations.

For these salts the atomic charges have been estimated by performing an integration over the topological atomic basins. The charge of about +2 e has been found both for Mn and Cl atoms and the ionic radius, estimated with the distance of the BCP from the nucleus (0.85 Å for Mn) agrees with the Mn^{2+} ionic radius of literature (0.80 Å) [38]. The charge of + 2 e on manga-

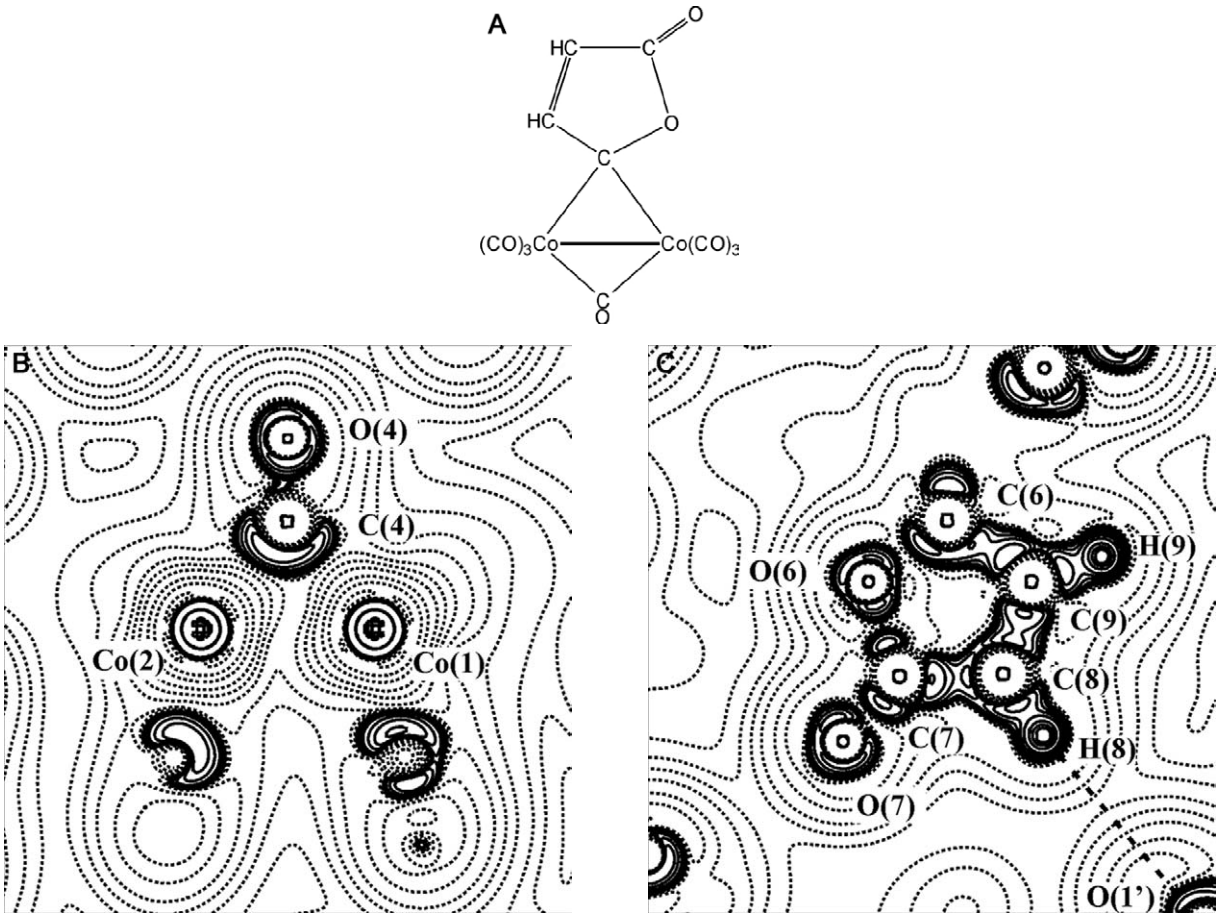

Fig. 4. (**A**) Scheme of the $Co_2(CO)_6(\mu\text{-}CO)(\mu\text{-}C_4O_2H_2)$ molecule. (**B**) Laplacian of the experimental charge density in the $Co_2(\mu\text{-}CO)$ plane and (**C**) in the *γ-lactonic* plane (an H···O interaction is evidenced for the triclinic phase). The contours are as in Fig. 1a.

Table 1
Co–Co distances and ρ_{BCP} in some organometallic compounds

Compound	Co–Co (Å)	ρ_{BCP} (e Å^{-3})	References
$Co_2(CO)_6(\mu\text{-}CO)(\mu\text{-}C_4O_2H_2)$ orthorhombic	2.4222(3)	0.76(6)	[32]
$Co_2(CO)_6(\mu\text{-}CO)(\mu\text{-}C_4O_2H_2)$ triclinic	2.4402(2)	0.46(2)	[33]
$Co_4(CO)_{11}As(Ph)_3$	2.528(8)	0.252(3)	[34]
$Co_2(CO)_6(AsPh_3)_2$	2.6430(2)	0.204(11)	[26]

nese is also in agreement with the corresponding result from the electron spectroscopy experiment on potassium permanganate [39]. A lower charge (nearly + 1 e) has been found in a theoretical study on MnO_4^- anion [40]. Furthermore, the experimental average VSCC radii are 0.75 Å for Cl, 0.42 Å for Mn, 0.65 Å for K and 0.48 Å for O atoms. A similar VSCC radius value has been obtained for the manganese atom in the $Mn_2(CO)_{10}$ complex, despite its different formal oxidation state.

We have also taken into account the debated topological characterization of the metal–metal bond. Our experimental and theoretical topological results on metal–metal bonds, together with those reported in the literature, are summarized in [41] and in Fig. 6. For comparison the topological indicators of the ionic NaF

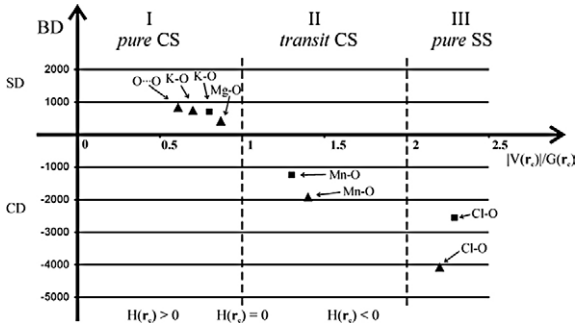

Fig. 5. BD of $KMnO_4$ and $KClO_4$ salts (BD = H_{BCP}/ρ_{BCP} where the units of H are kJ mol^{-1} per atomic unit volume and units of ρ are e Å^{-3}) as a function of $|V_{BCP}|/G_{BCP}$. Triangles and squares refer to experimental and theoretical data, respectively.

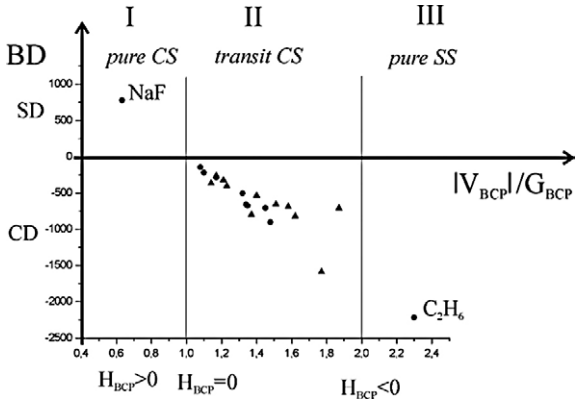

Fig. 6. Bond Degree (BD = H_{BCP}/ρ_{BCP} where the units of H are kJ mol^{-1} per atomic unit volume and units of ρ are e Å^{-3}) as a function of $|V_{BCP}|/G_{BCP}$. Dots in *transit* CS zone refers to theoretical values in bulk metals; triangles represent both theoretical and experimental values for metal–metal bonds in organometallic complexes [41].

and of the covalent C_2H_6 are also reported. In the same Figure the theoretical topological parameters of bulk metals are illustrated [42,43].

The metal–metal bonds lie in the *transit* CS region, with topological features intermediate between typical covalent and ionic bonds for both polynuclear complexes and bulk metals. They have positive $\nabla^2\rho_{BCP}$, low ρ_{BCP}, a little CD and a flat charge density in the valence region. The index of flatness f is defined as

$$f = \rho^{min}/\rho^{max}_{BCP}$$

where ρ^{min} is the absolute minimum of $\rho(\mathbf{r})$ and ρ^{max} is the maximum $\rho(\mathbf{r})$ found among BCPs [44]. f Approaches unity for metals and goes to zero for non-metals (e.g., for alkaline metals f = 0.89–0.95 and for alkaline earth metals f = 0.64–0.75). For the Co–Co–C rings in the two $Co_2(CO)_6(\mu\text{-}CO)(\mu\text{-}C_4O_2H_2)$ polymorphs, the ratio f between the ρ^{min} of the ring CP and the ρ^{max}_{BCP} of the Co–Co bond is 0.97 av., while for the *lactone* ring (all covalent bonds) it is 0.21 av. Unfortunately, no data are available at the present for ring or cage critical points of other organometallic complexes.

Thus, using the topological parameters now at our disposal, we can conclude that *the metal–metal bond in the polynuclear complexes has the same nature as in the bulk metals*. Differently, other authors, on the basis of some topological parameters at the BCP (in particular $H_{BCP} < 0$) and of 'common chemical sense', classify the metal–metal bond as a 'genuine covalent bond' [29,45]. We think instead that the metal–metal bond in complexes has its own unique features, similar to those of bonds in bulk metals.

4. Conclusions

The multipolar refinement, based on low temperature diffraction data, supplies accurate charge density distributions. The QTAIM is a useful tool to analyze the multipolar charge density and to well characterize the intra and inter-molecular bonds even in presence of first-row transition metals. In particular, for some organometallic compounds it has contributed to the long-debated discussion on the existence of a direct metal–metal bond and to the nature of this bond.

We have applied tentatively the classification proposed by Espinosa et al. to several interatomic bond types and it seems a powerful mean for evidencing the charge density features of bonds. In particular this classification together with the topological parameters of metal–metal bonds has allowed to recognize the unique features of these bonds.

Another tool at our disposal is the analysis of VSCC maxima and minima of bonded atoms. For example, it has allowed to associate the metal–ligand bond to a 'dative' bond. However, the analysis of this bond is still is in progress.

Note added in proof

A QTAIM analysis of $Ru_3(CO)_{12}$ was published in the meantime (G. Gervario, R. Bianchi, D. Marabello, Chem. Phys. Lett. 407 (2005) 18.

References

[1] T.S. Koritsanszky, P. Coppens, Chem. Rev. 101 (2001) 1583–1627.
[2] R.F.W. Bader, Atoms in Molecules – A Quantum Theory, Oxford University Press, Oxford, UK, 1984.
[3] R.F. Stewart, Acta Crystallogr. A 32 (1976) 565.
[4] N.K. Hansen, P. Coppens, Acta Crystallogr. A 34 (1978) 909.
[5] R.F. Stewart, M.A. Spackman, C. Flensburg, VALRAY, versions 1995–2000.
[6] T. Koritsanszky, S.T. Howard, T. Richter, P. Macchi, A. Volkov, C. Gatti, P.R. Mallinson, L.J. Farrugia, Z. Su, N.K. Hansen, XD—A Computer Program Package for Multipole Refinement and Topological Analysis of Charge Densities from Diffraction Data, 2003.
[7] C. Gatti, TOPOND-96,98: an electron density topological program for systems periodic in N (N = 0–3) dimensions, User's Manual; CNR-ISTM, Milano, Italy, 1999.
[8] D.A. Kirzhnits, Sov. Phys. JETP 5 (1957) 64.
[9] Y.A. Abramov, Acta Crystallogr. A 53 (1997) 264.
[10] E. Espinosa, E. Molins, C. Lecomte, Chem. Phys. Lett. 285 (1998) 170.
[11] D. Cremer, E. Kraka, Croat. Chem. Acta 57 (1984) 1259.
[12] D. Cremer, E. Kraka, Angew. Chem. Int. Ed. Engl. 23 (1984) 67.
[13] E. Espinosa, I. Alkorta, J. Elguero, E. Molins, J. Chem. Phys. 117 (2002) 5529.
[14] R. Bianchi, G. Gervasio, G. Viscardi, Acta Crystallogr. B 54 (1998) 66.
[15] R. Destro, R.E. Marsh, R. Bianchi, J. Phys. Chem. 92 (1988) 966.
[16] R. Destro, R. Bianchi, G. Morosi, J. Phys. Chem. 93 (1989) 4447.
[17] R. Bianchi, C. Gatti, V. Adovasio, M. Nardelli, Acta Crystallogr. B 52 (1996) 471.
[18] M. Catti, G. Gervasio, S.A. Mason, J. Chem. Soc., Dalton Trans. (1977) 2260.
[19] G. Gervasio, S.A. Mason, L. Maresca, G. Natile, Inorg, Chem. 25 (1986) 2207.
[20] E. Gatto, G. Gervasio, D. Marabello, E. Sappa, J. Chem. Soc., Dalton Trans. 10 (2002) 1448.
[21] G. Gervasio, R. Rossetti, P.L. Stanghellini, G. Bor, Inorg. Chem. 21 (1982) 3781.
[22] S. Vastag, G. Gervasio, D. Marabello, G. Szalontai, L. Markó, Organometallics 17 (1998) 4218.
[23] R. Bianchi, G. Gervasio, D. Marabello, Chem. Commun. (1998) 1535.
[24] R. Bianchi, G. Gervasio, D. Marabello, Inorg. Chem. 39 (2000) 2360.
[25] M. Martin, B. Rees, A. Mitschler, Acta Crystallogr. B 38 (1982) 6.
[26] P. Macchi, D.M. Proserpio, A. Sironi, J. Am. Chem. Soc. 120 (1998) 120.
[27] G. Jansen, M. Schubart, B. Findeis, L.H. Gade, I. Scowen, M. McPartlin, J. Am. Chem. Soc. 120 (1998) 7239.
[28] R. Bianchi, G. Gervasio, D. Marabello, XXVIth Congresso Nazionale AIC, 1–4 September 1996.
[29] L.J. Farrugia, P.R. Mallinson, B. Stewart, Acta Crystallogr. B 59 (2003) 234.
[30] A.A. Low, K.L. Kunze, P.J. MacDougall, M.B. Hall, Inorg. Chem. 30 (1991) 1079 (and references therein).
[31] R. Bianchi, G. Gervasio, D. Marabello, XVIIIth ECM, Praha, 15–20 August 1998.
[32] R. Bianchi, G. Gervasio, D. Marabello, Helv. Chim. Acta 84 (2001) 722.
[33] R. Bianchi, G. Gervasio, D. Marabello, Acta Crystallogr. B 57 (2001) 638.
[34] P. Macchi, L. Garlaschelli, S. Martinengo, A. Sironi, J. Am. Chem. Soc. 121 (1999) 10428.
[35] P. Macchi, L. Garlaschelli, A. Sironi, J. Am. Chem. Soc. 124 (2002) 14173.
[36] M. Finger, J. Reinhold, Inorg. Chem. 42 (2003) 8128.
[37] D. Marabello, R. Bianchi, G. Gervasio, F. Cargnoni, Acta Crystallogr. A 60 (2004) 494.
[38] R.D. Shannon, Acta Crystallogr. A 32 (1976) 751.
[39] F. Reinert, P. Steiner, S. Hüfner, J. Magn. Mater. 140–144 (1995) 177.
[40] H. Nakai, Y. Ohmori, H. Nakatsuji, J. Chem. Phys. 95 (1991) 8287.
[41] G. Gervasio, R. Bianchi, D. Marabello, Chem. Phys. Lett. 387 (2004) 481.
[42] Y. Aray, J. Rodriguez, D. Vega, J. Phys. Chem. B 104 (2000) 4608.
[43] W. Uhl, S. Melle, G. Frenking, M. Hartmann, Inorg. Chem. 40 (2001) 750.
[44] P. Mori-Sanchez, A.M. Pendás, V. Luaña, J. Am. Chem. Soc. 124 (2002) 14721.
[45] P. Macchi, A. Sironi, Coord. Chem. Rev. 238–239 (2003) 383.